We are IntechOpen,
the world's leading publisher of
Open Access books
Built by scientists, for scientists

6,900
Open access books available

186,000
International authors and editors

200M
Downloads

Our authors are among the

154
Countries delivered to

TOP 1%
most cited scientists

12.2%
Contributors from top 500 universities

CLARIVATE ANALYTICS
BOOK CITATION INDEX
INDEXED

WEB OF SCIENCE™

Selection of our books indexed in the Book Citation Index
in Web of Science™ Core Collection (BKCI)

Interested in publishing with us?
Contact book.department@intechopen.com

The UWB Channel in Medical Wireless Body Area Networks (WBANs)

Carlos Pomalaza-Ráez and Attaphongse Taparugssanagorn

Additional information is available at the end of the chapter

1. Introduction

UWB is a technology that has several advantages when considered for a Wireless Body Area Network (WBAN). A WBAN is a network with its communications devices in very close proximity to the human body. In medical applications these devices are connected to sensors that can monitor vital signs such as ECG, temperature, and mobility. A WBAN allows for the remote monitoring of a patient's health minimizing the number of cables needed. The monitoring of vital signals usually require a relatively low data-rate which in the case of UWB translates into very small transmitting power, long battery life, and less potential side effects caused by electromagnetic radiation. All of these features are very desirable for devices that are close to the body and meant to be used for extended periods of time.

The human body is a complex structure and human tissues have different electrical properties which affect the propagation of electromagnetic signals. Moreover, as the human body moves, the characteristics of the radio links changes, e.g. the link from the chest to a wrist will change from line-of-sight to non-line-of-sight as a person walks.

To be able to design and develop UWB devices that can interface with WBANs it is then necessary to understand well the characteristics of the radio propagation channel at UWB frequencies and in close proximity to the human body. UWB measurements around a human body have been carried out by several researchers (Fort et al., 2006). There is however a lack of measurements, and subsequent analysis, carried out in real medical environment such as hospitals. The studies described in this chapter focus on scenarios most likely to be found in medical applications and as such they do not assume a large amount of antennas in close proximity to the skin. Among the several issues taken into account are the effects of mobility, and the interaction of the UWB signal with medical implants.

2. Hospital scenarios

Fig. 1 shows a common hospital room scenario. Medical information is collected by sensors on the patient's body. The sensors are interfaced to a WBAN which transmit the information to be displayed on a bedside monitor. This information can also be transmitted to another hospital location for remote monitoring, e.g. a nurse's station. The radio links present in this type of scenario include the ones between sensor nodes (link A1), the links between the sensors and a gateway node (links A2), and the links from wireless devices carried by visitors or healthcare professionals (link A3). Other possible radio links are from the gateway to wireless networks such as 802.11 b/g/n and WiMAX.

Figs. 2 and 3 show real hospital scenarios where measurements described in this chapter were taken (Taparugssanagorn et al. 2010). A regular hospital room is shown in Figure 2. This room's dimensions are: 6.3 m x 7.2 m x 2.5 m. A surgery room, with dimensions 6 m x 4.7 m x 2.5 m, is shown in Figure 3. Both radio links A1 and A2 were measured in each room. Within the hospital several scenarios were considered. Table 1 summarizes the measurements and scenarios in this study. A detailed description of the various experiments and the results can be found in (Taparugssanagorn et al. 2010). To illustrate the experiments and analyses performed the case of a subject standing in hospital room is discussed in more detail in the next section.
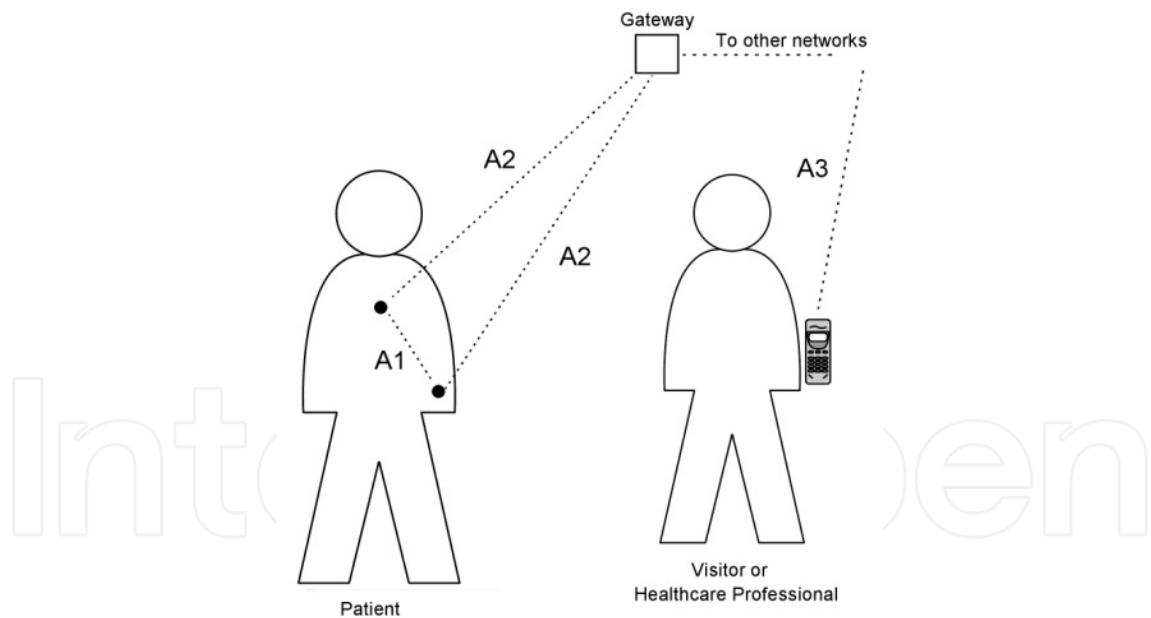

Figure 1. A typical hospital room scenario: A1 is a link between sensor nodes, A2 is a link between a sensor node and a gateway, and A3 is a link to other wireless networks.

To measure the A1 link, the receive (Rx) antenna was located at the centre of the front torso and the transmit (Tx) antenna was placed on the left wrist. These locations are comfortable for most patients and are also convenient places for sensors such as electrodes in the chest areas to generate an electrocardiogram (ECG) and a pulse oximeter on a finger trip to monitor the patient's oxygenation. To measure the A2 link, the Rx antenna was placed on a

2 m high pole located 2 m away from the subject and the Tx antenna was on the left side of the waist.

Figure 2. Floor plan of a regular hospital room.

Figure 3. Floor plan a surgery room

Environment	Scenarios	
Regular Room	Subject Standing Links A1 and A2	Subject Lying Links A1 and A2
Surgery Room	Subject Lying 2 people walking around the bed Links A1 and A2	Subject Lying 2 people walking around the bed, one of them is using a mobile phone Links A1 and A2

Table 1. Measurements and scenarios.

3. Channel measurements and models

The measurements were carried out using an Agilent 8270ES vector network analyzer (VNA). The antennas used were SkyCross SMT-3TO10M-A. These antennas are linearly polarized and azimuthally omnidirectional. The cables used were 5 m long SUCOFLEX RF with 7.96 dB loss. The data acquisition system included a computer with LabVIEW™ software. The VNA was operated in a transfer function measurement mode, where Port 1 and Port 2 are the transmitting and receiving ports respectively, as seen in Fig. 4.
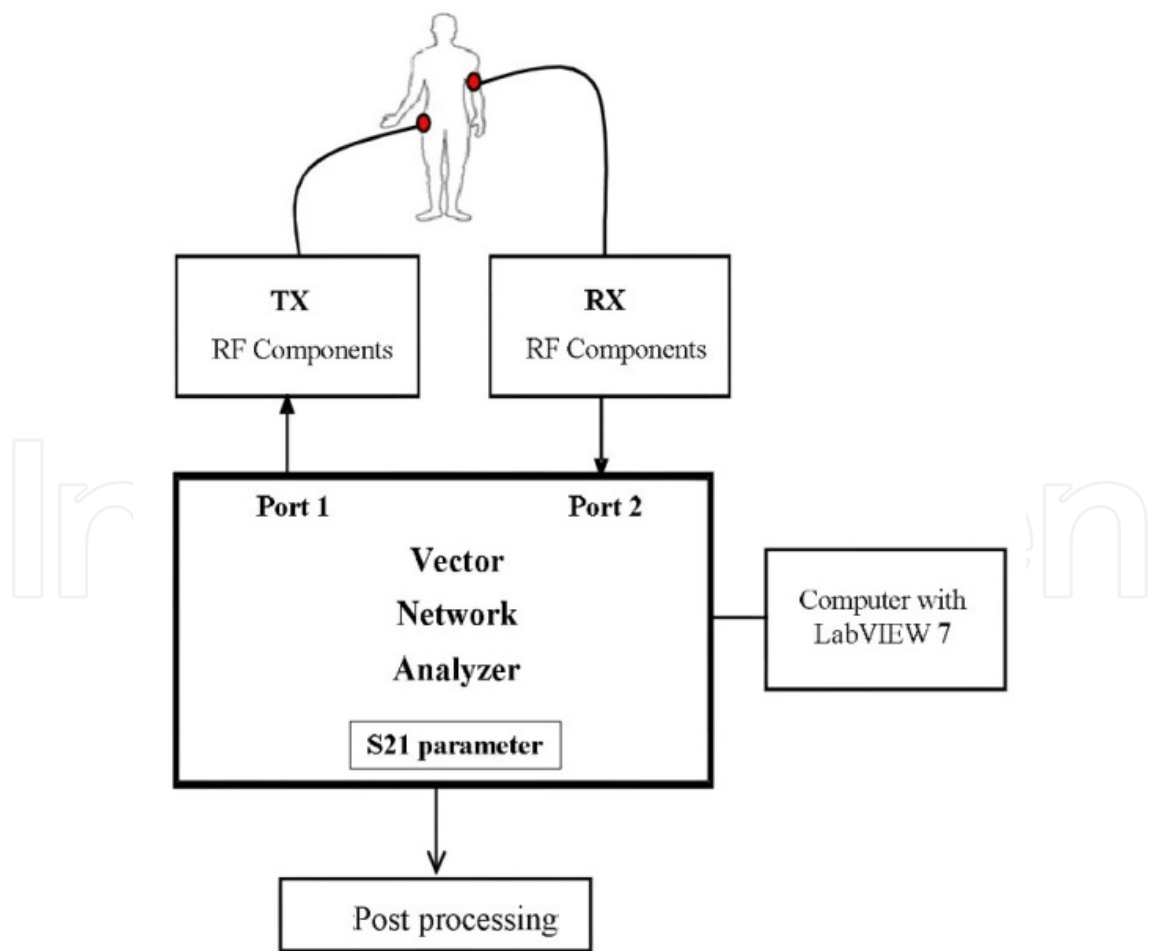

Figure 4. Measurement setup

This setup corresponds to a measurement of the S21 parameter where the device under test (DUT) is the radio channel. The range of the frequency spectrum covered was from 3.1 GHz to 10.6 GHz. For each experiment setup 100 frequency responses were measured. The measurement parameters are summarized in Table 2.

Parameter	Value
Frequency range	3.1 to 10.6 GHz
Bandwidth	6.9 GHz
VNA IF bandwidth	3.0 kHz
Number of samples per sweep	1601
Maximum detectable delay	231 ns
Sweep time	800 ms
Average noise floor	- 120 dBm
Transmit power	0 dBm
Tx and Rx cables' loss	7.96 dB

Table 2. Measurement parameters

The measured transfer function frequency values were converted to the time domain (channel impulse response) using an inverse Fast Fourier Transform. A Hamming window was used to reduce sidelobes.

3.1. Channel impulse response

Fig. 5 shows the average of the channel impulse response, corresponding to link A1, when the subject is standing in the hospital room shown in Fig. 2.

The effect of the human body and the environment can be clearly differentiated. These results are significantly different than the ones obtained in an empty hospital room (Hentilä et al, 2005). In Fig. 5 the first region of the IR shows a fast decay of the energy during the first 5-6 ns due to the effects of the human body. The decay of the second region in the response is slower and contains the diffuse multipath components and a few subclusters caused by the reflections coming from the room. In this particular case the first of such subclusters, arriving at around 8 ns, is due to a measuring equipment (VNA) which was located 1.3 m in front of the subject when is standing.

For each particular hospital scenario listed in Table 1 the measurements obtained share the general characteristics shown in Fig. 5.

Fig. 6 corresponds to the case when the subject is lying down on bed in a hospital room. Fig. 7 corresponds to the case when the subject is lying down on a bed in a surgery room and two other people are randomly walking around the bed. The Least Squares (LS) fitted lines shown in these figures are used to model the variability of the amplitudes as described in Section 3.2.
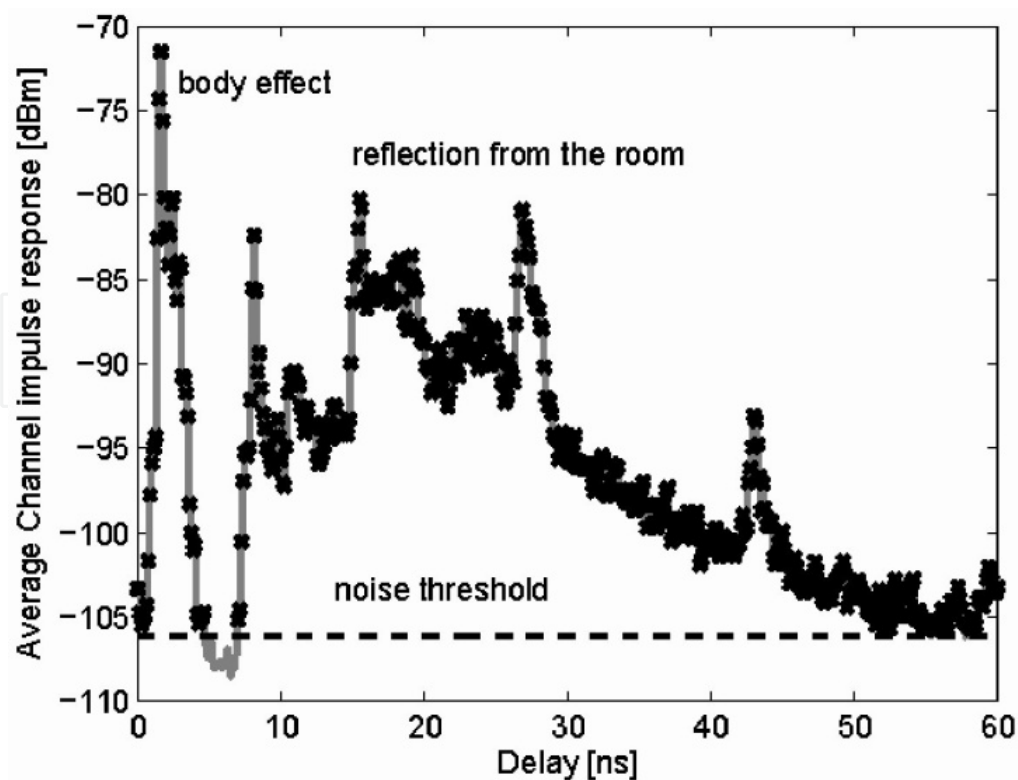
Figure 5. Average channel impulse response of the radio link A1. The subject is standing in a regular hospital room.
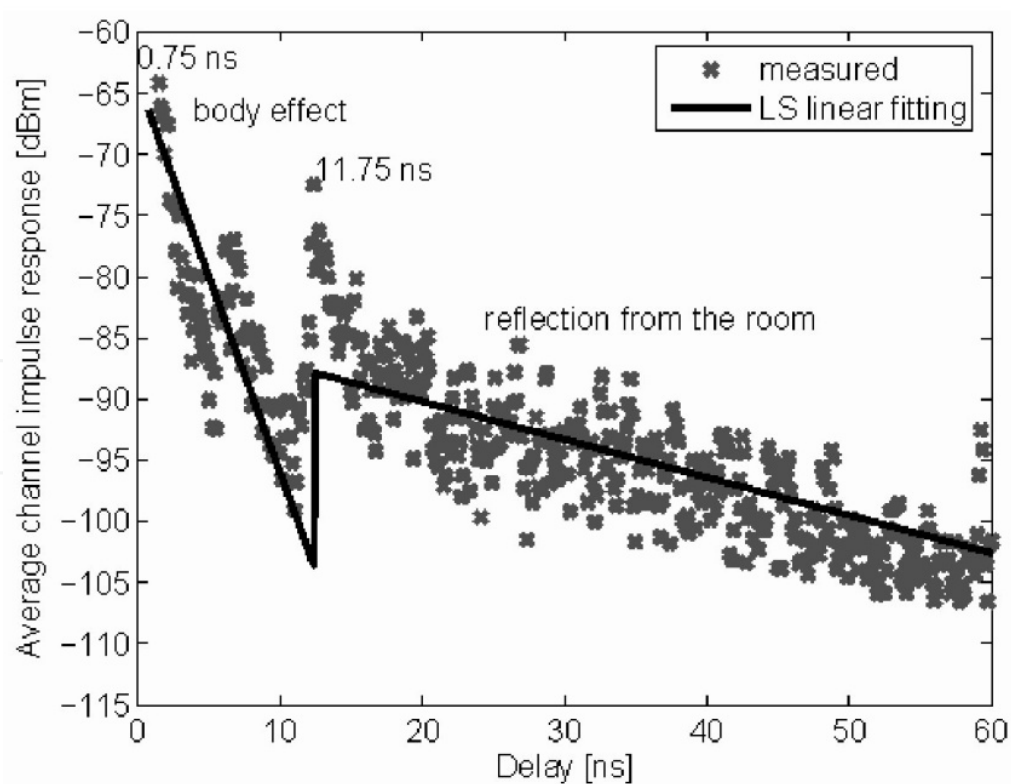

Figure 6. Average channel impulse response of the radio link A1. The subject is lying down on a bed in a regular hospital room.
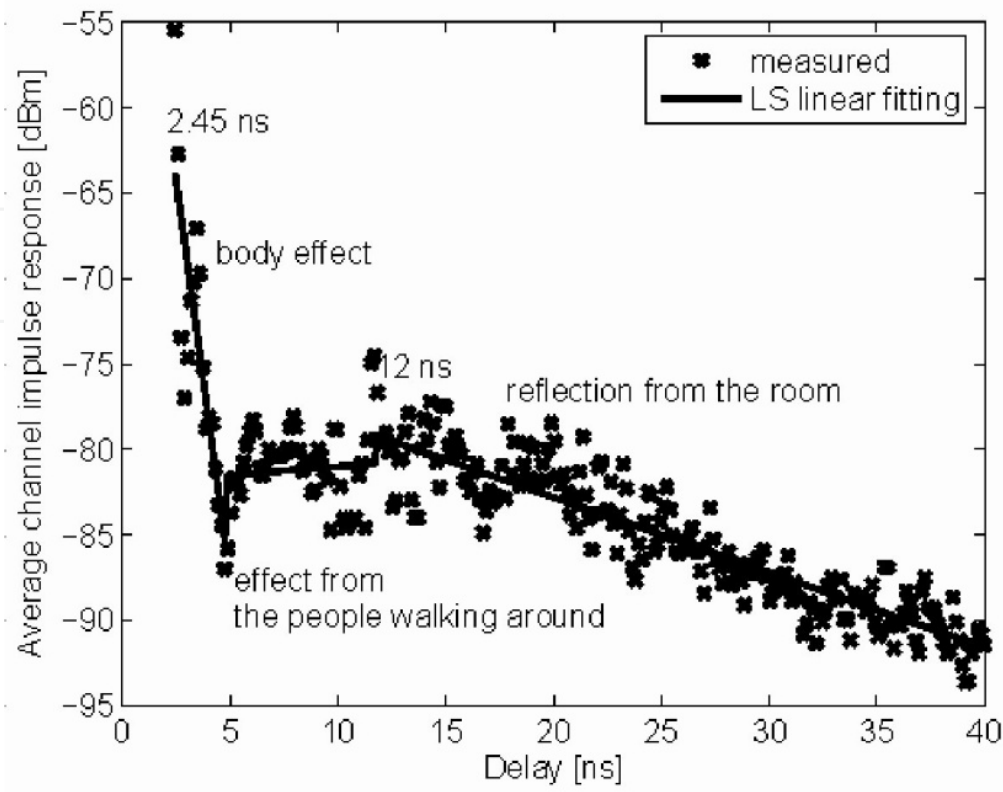
Figure 7. Average channel impulse response of the radio link A1. The subject is lying down on a bed in a surgery room and two other people are randomly walking around the bed.

3.2. Channel models

Once a set of measurements have been obtained they are used to estimate the parameters of a common mathematical representation of communications channels, a tapped delay line.

$$h(\tau) = \sum_{l=0}^{L-1} a_l \delta(\tau - \tau_l) \exp(j\phi_l) \tag{1}$$

In equation (1) L is the number of paths. For the ith path, a_l is the signal amplitude, τ_l is the arrival time, and ϕ_l is the phase. For the case shown in Fig. 5 (when the subject is standing in a regular hospital room) it is more appropriate to consider two regions for the modeling of the signal clusters, each with it is own set of distributions for the characterization of the amplitudes decays and intearrival times.

3.2.1. Exponentially decaying factor

As illustrated in Fig. 8, the values of a_l in equation (1) can be approximated by two exponential decaying functions, one for each region. Using a least squares (LS) method these functions (when expressed in dB) are best fitted with a Rician factor γ_0 and an exponential decaying factor Γ (equation (2)).
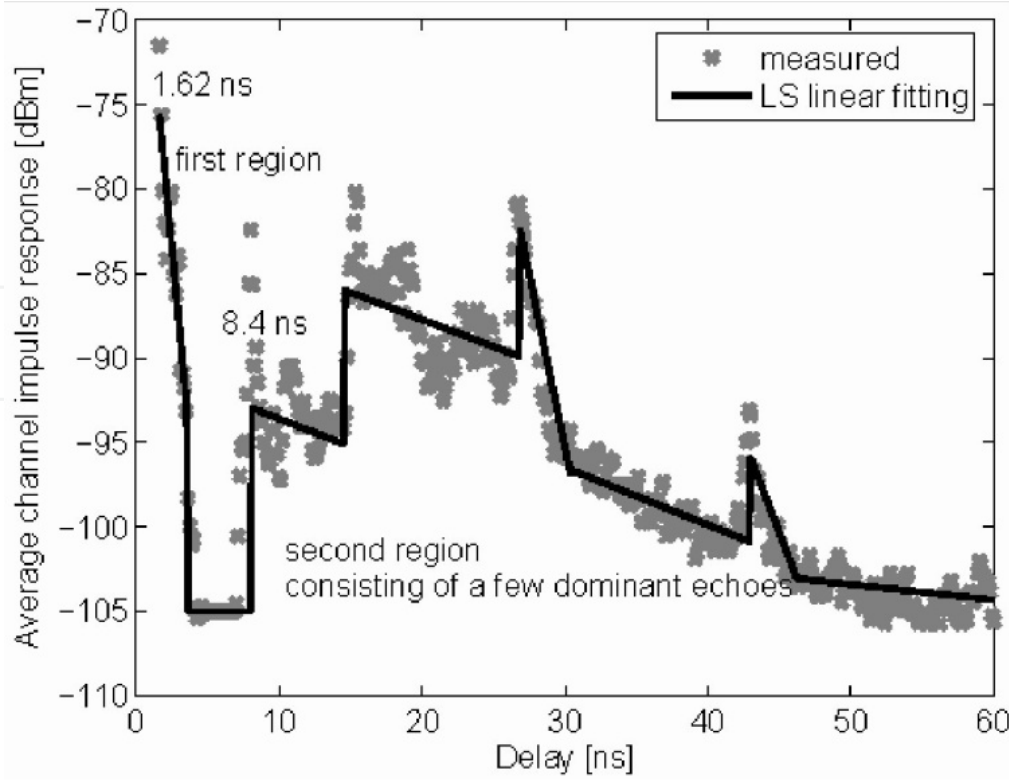
Figure 8. Least Squares fitting of the average channel response of the radio link A1. The subject is standing in a regular hospital room.

$$10 \log_{10} |a_l| = \begin{cases} 0, & l = 0 \\ \gamma_{01} + 10 \log_{10} \left(\exp \left(\frac{-t_l}{\Gamma_1} \right) \right), & 1 \leq l \leq l_1 \\ \sum_{m=1}^{M} \left(\gamma_{02m} + 10 \log_{10} \left(\exp \left(\frac{-t_l}{\Gamma_{2m}} \right) \right) \right), & l_2 \leq l \leq L-1 \end{cases} \quad (2)$$

where $\gamma_{01}, \gamma_{02m}, \Gamma_1$, and Γ_{2m} are the corresponding parameters for each region. l_1 and l_2 are the index for the last path of the first region and the first path of the second region respectively.

For the measurements shown in Fig. 5 the values of the function's parameters for the first region are $\gamma_{01} = -61$ dB and $\Gamma_1 = 1.11$. For the second region the values are $\gamma_{02m} = \{-91, -82, 19, -87, -6, -99\}$ dB and $\Gamma_{2m} = \{30.30, 31.25, 2.44, 29.41, 4.55, 108.70\}$.

3.2.2. Amplitude variation and path arrival times

Amplitude variations for each region have been modelled as a log-normal distribution with zero-mean and standards deviations $\sigma_1 = 2.45$ and $\sigma_{2m} = \{2.07, 2.21, 1.62, 1.44, 1.20, 0.91\}$.

Path arrival times $(t_l - t_{l-1})$, i.e. the time difference between consecutive arrival paths, have been modelled, using the LS method, with the following exponential distributions.

$$p(t_l|t_{l-1}) = \begin{cases} \lambda_1 \exp(-\lambda_1(t_l - t_{l-1})), & 1 \leq l \leq l_1 \\ \lambda_2 \exp(-\lambda_2(t_l - t_{l-1})), & l_2 \leq l \leq L - 1 \end{cases} \tag{3}$$

The path arrivals can then be modelled as a Poisson process.

$$p(L) = \frac{\mu_L \exp(\mu_L)}{L!} \tag{4}$$

For the case discussed in this section $\lambda_1 = 0.269$ and $\lambda_2 = 0.163$ and the value of μ_L is 324.

4. Effect of body motion

UWB signals are very sensitive to absorption by objects that have a high percentage of water, such as human bodies and plants. It is then expected that WBANs using UWB technology will have particular characteristics when the human body is in motion. To study the effects of motion, measurement while a subject is walking (as shown in Fig. 9) have been performed (Taparugssanagorn et al. 2009).

A real-time measurement and processing of the channel fluctuations due to a body in motion is not possible with the equipment described in Section 3. Instead, a pseudo-dynamic method was used, where each position of the walking cycle shown in Fig. 9 was kept still for the whole time it takes to take 100 snapshots. The average of the magnitude of the channel impulse response is shown in Fig. 10.
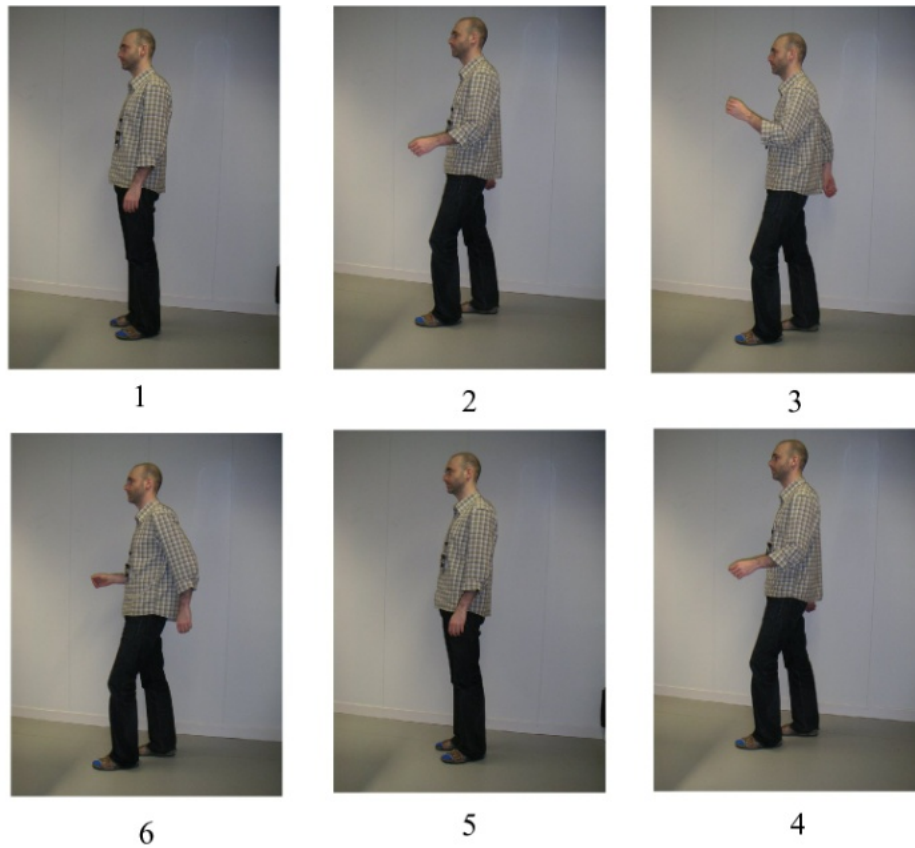

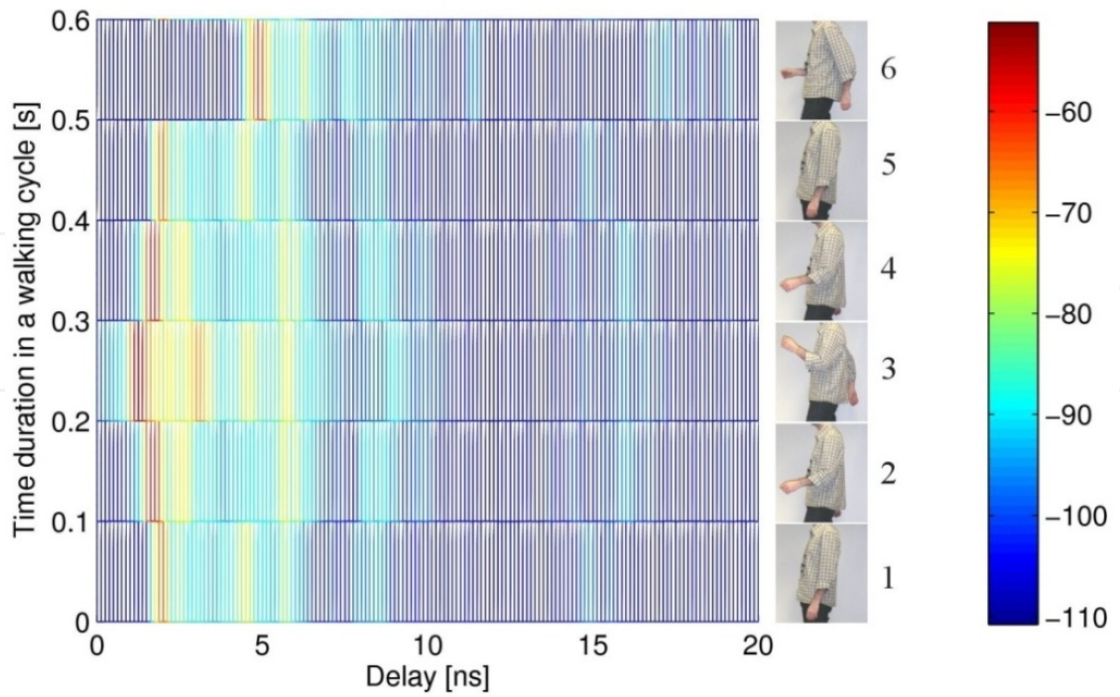**Figure 9.** Positions within a walking cycle

Figure 10. Magnitude of the channel impulse response for each position of the walking cycle.

These experimental results indicate that the arm movements have a significant impact on the radio link A1 (Tx antenna on the left wrist and Rx antenna in the center of the front torso). For instance, when the hand moves to position three the strongest path arrives earlier than in the other positions due to the shorter distance between the antennas. There are also more significant paths due to the interaction of the electromagnetic waves with of the arm and the shoulder. The shadowing of the signal due to blocking by the body is evident in position six, where the left hand moves to the lowermost location.

Fig. 11 provides an alternative view of the channel impulse response where the delay of the most prominent peak is clearly shown (Taparugssanagorn et al. 2011).

To evaluate the delay dispersion within the channel the root mean square (RMS) delay spread τ_{RMS} is estimated. The τ_{RMS} is defined as,

$$\tau_{RMS} = \sqrt{\frac{\sum_{i=0}^{L-1}(\tau_i-\tau_m)^2|h(\tau_i)|^2}{\sum_{i=0}^{L-1}|h(\tau_i)|^2}} \tag{5}$$

where τ_m is the mean excess delay defined as,

$$\tau_m = \frac{\sum_{i=0}^{L-1}\tau_i|h(\tau_i)|^2}{\sum_{i=0}^{L-1}|h(\tau_i)|^2} \tag{6}$$

$h(\tau)$ is the channel impulse response, L is the number of paths and τ is the delay. For the case discussed here the estimates for mean and the standard deviation of τ_{RMS} are 0.1371 ns and 0.0670 ns respectively. Also the probability distribution function that best fits the variations of the amplitude is the Weibull distribution.
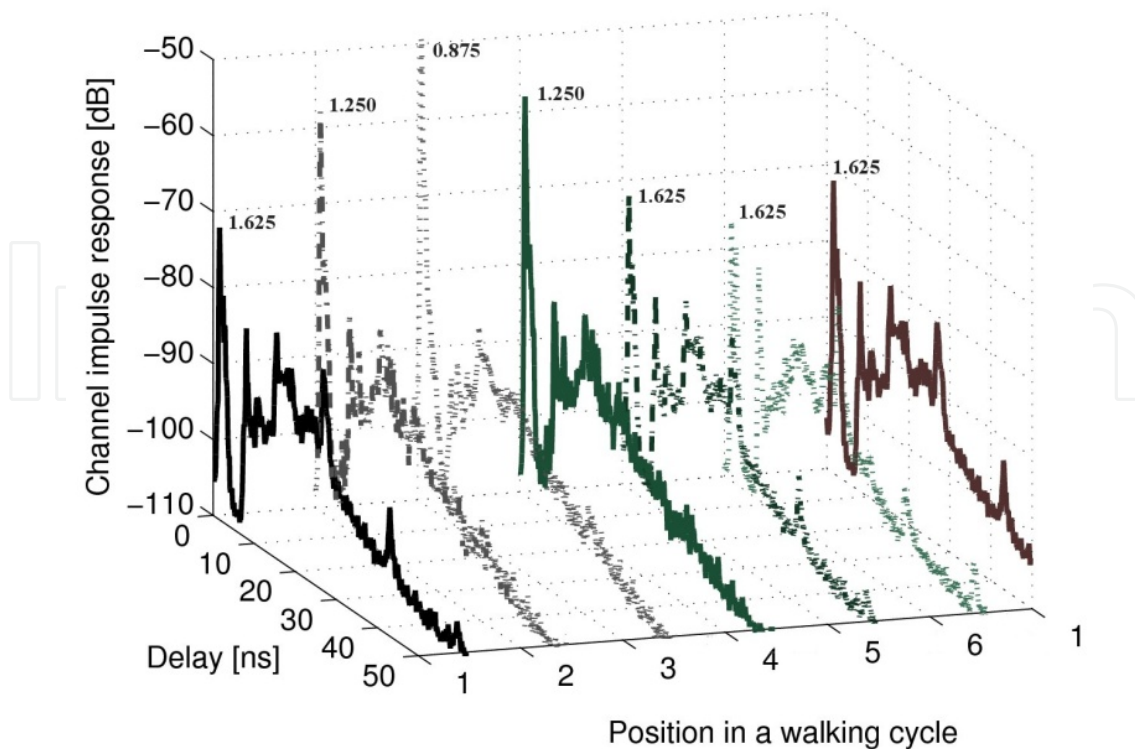
Figure 11. Channel impulse response (link A1) for each position of the walking cycle.

The results presented in this and in the previous section highlight the importance of properly understand and model the UWB channel when designing physical and Medium Access Protocols (MAC) to be used in medical applications (Viittala et al., 2009).

5. UWB radar in medical applications

The potential use of UWB technology goes beyond transmitting information, collected by sensors, to a control station. The nature of the UWB signal is such that it can be used as in common radar applications, e.g. to detect and estimate dynamic parameters of an object. Fig. 12 shows the channel impulse responses for the case of subjects with and without an aortic valve implant (Taparugssanagorn et al. 2009). The Rx antenna was located at the middle of the front torso and the Tx antenna close to the heart, 10 cm away from the Rx antenna. P200 BroadSpec™ UWB antennas were used for this experiment.

It apparent that the responses are different, i.e. the one corresponding to the subject with an aortic implant has lower peaks. A possible explanation for the difference in the responses is the scattering caused by the metallic (titanium alloy) valve. Subsequent simulation studies carried out using a 3D immersive visualization environment has confirmed this type of results (Yang et al., 2011). Further investigations could lead to the use of the response to infer the nature of the implant behaviour.

The use of UWB signals to directly monitor vital signs is currently a very active research area. Thus for example, the estimation of the breathing rate and the heart beat frequency has been studied in (Lazaro et al., 2010). Using a mathematical model of the human body as

related to its effect on the propagation of the UWB signals the feasibility of medical diagnosis using UWB radar technology has been assessed in (Pancera et al., 2011).
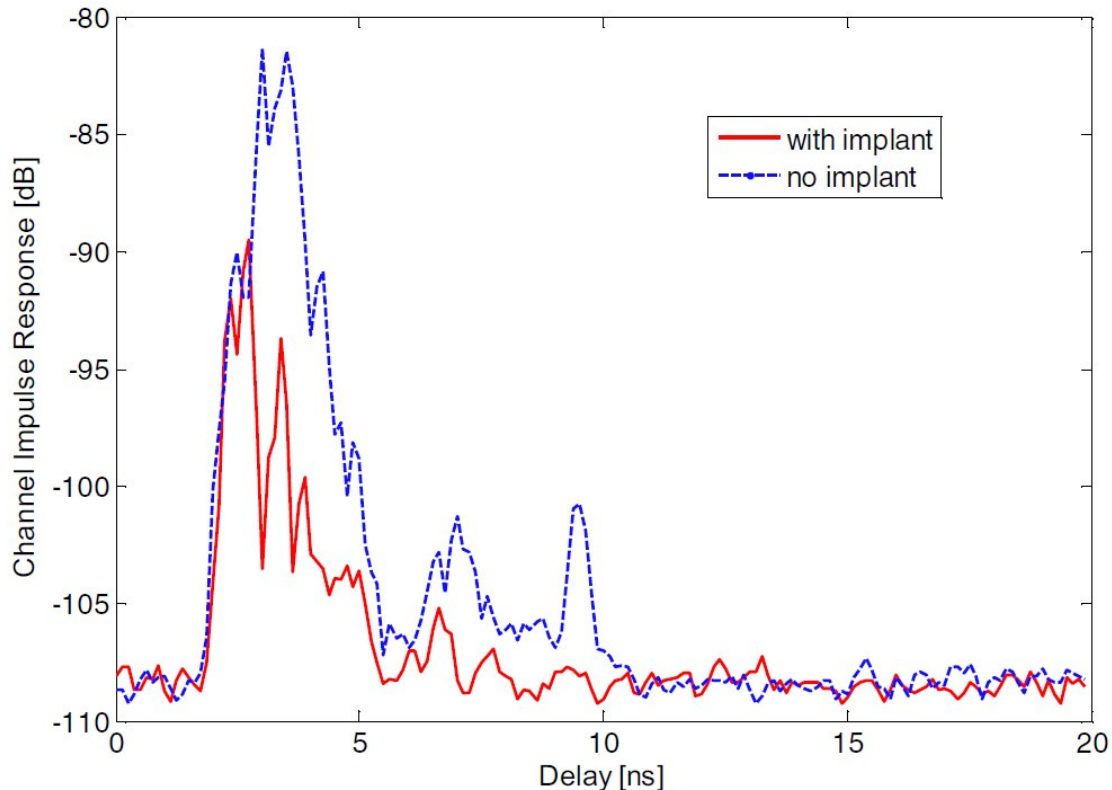

Figure 12. Average channel impulse response for subjects with and without aortic valve implant.

In summary UWB technology can be used not only to transmit information collected by sensors such as ECG electrodes and pulse oximeters but also to actively monitor vital signals and the behaviour of artificial implants.

6. Standards

For WBANs to become widely adopted it is important to have standards. The IEEE 802.15 group of standards focuses on short range communications, low complexity, and low power consumption making them suitable for use in WBANs. Two standards from this group have specifically addressed the use of UWB technology with medical applications in mind. This section describes UWB features of the IEEE 802.15.4 standard of the recently approved IEEE 802.15.6 standard.

The IEEE 802.15 task group 6 (TG6) developed a UWB channel model as part of the process of developing the IEEE 802.15.6 standard (Yazdandoost & Sayrafian-Pour, 2009). A comparison of the IEEE 805.15.6 channel model and the one described in this chapter can be found in (Viittala et al., 2009).

6.1. IEEE 802.15.4

The IEEE 802.15.4 standard and the industrial consortium supporting it, the ZigBee alliance, are widely used in wireless sensor networks (WSNs) applications. The IEEE 802.15.4 standard provides alternative physical layers for devices with precision ranging and extended range (IEEE Std 802.15.4, 2011). The UWB physical layer option of this standard provides for features that are desirable in medical applications such as very low power. The data rates supported are 110 kb/s, 851 kb/s, 1.70 Mb/s, 6.81 Mb/s, and 27.24 Mb/s. Whereas this standard has desired features to be used in medical applications it does not support the levels of safety, quality of service, and security features wanted in many of those applications. Thus, the remainder of this section deals with the IEEE 802.15.6 standard which has features specifically designed to support medical applications.

6.2. IEEE 802.15.6

The final version of this standard has been recently released (IEEE Std 802.15.6, 2012). It specifically deals with wireless communications in the vicinity of, or inside, a human body. It uses existing industrial scientific medical (ISM) bands and other bands. It allows devices to operate on very low transmit power and thus minimizes the specific absorption rate (SAR) into the body as well as increases the battery life. It also supports data rates up to 10 Mbs, quality of service (QoS) and it provides for strong security. The standard takes into account the use of portable antennas in the presence of a human body.

The default mode should support impulse radio UWB (IR-UWB) with a mandatory uncoded data rate of 487.5 kbs. It should also support, as optional PHY, wideband frequency modulation UWB (FM-UWB) with a mandatory uncoded data rate of 250 kbs.

The standard provides specifications for the physical layer (PHY) and the medium access control (MAC) sublayer. Three PHYs are supported by the IEEE 802.15.6 as illustrated in Fig. 13.
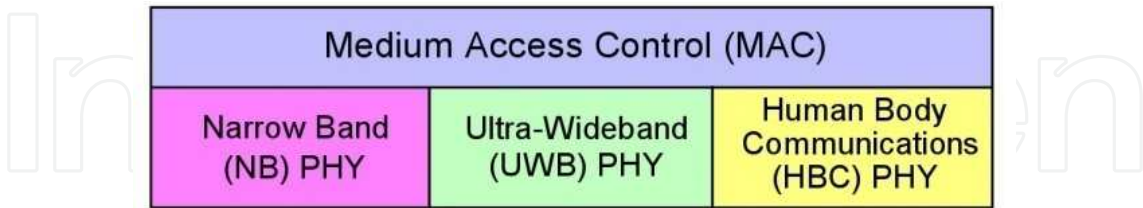

Figure 13. IEEE 802.15.6 MAC and PHY layers

The UWB PHY layer constructs the PHY layer protocol data unit (PPDU) by concatenating the synchronization header (SHR), physical layer header (PHR), and the physical layer service data unit (PSDU). The SHR has two parts. The first part is a preamble, intended for timing synchronization, packet detection, and frequency offset recovery. The second part is the start-of-frame delimiter (SFD). Kasami sequences of length 63 are used to build the preamble. The usage of preamble sequences improves coexistence of WBANs and interference mitigation as different WBANs use different preamble sequences. The PPUD is

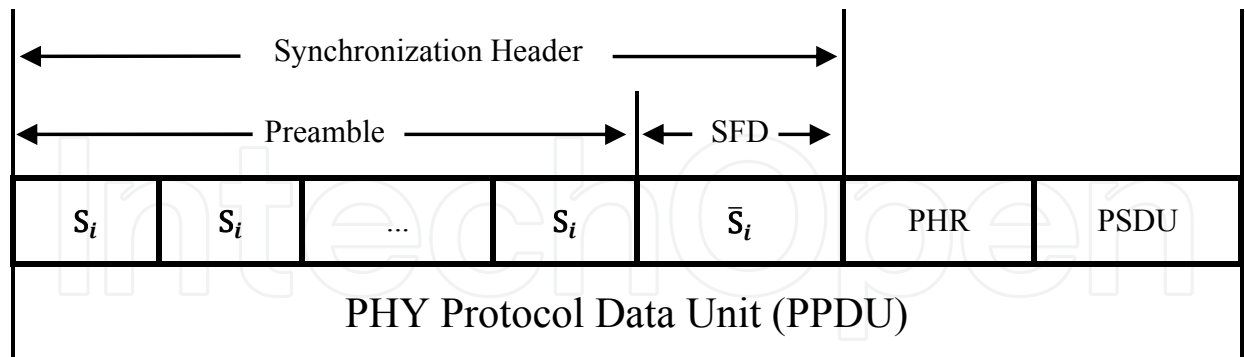illustrated in Fig. 14. The PPUD bits are converted into RF signals for transmission in the wireless medium.

Figure 14. IEEE 802.15.6 UWB physical layer protocol data unit (PPDU)

The PHR contains information about the data rate of the PSDU. The coded bit rates supported are shown in Table 3.

UWB - PHY	Data rate 0 (kb/s)	Data rate 1 (kb/s)	Data rate 2 (kb/s)	Data rate 3 (kb/s)	Data rate 4 (kb/s)	Data rate 5 (kb/s)	Data rate 6 (kb/s)	Data rate 7 (kb/s)
On-Off	394.8	789.7	1579	3159	6318	12636		
DBPSK/DQPSK	487	975	1950	3900	7800	15600	557	1114
FM	202.5							

Table 3. IEEE 802.15.6 UWB-PHY coded bit rates.

According to the IEEE 802.15.6 standard all nodes and hubs are organized into logical sets called body area networks (BANs) as illustrated in Fig. 15. There is one and only one hub in a BAN. The number of nodes in a BAN ranges from zero to nMaxBANSize=64.
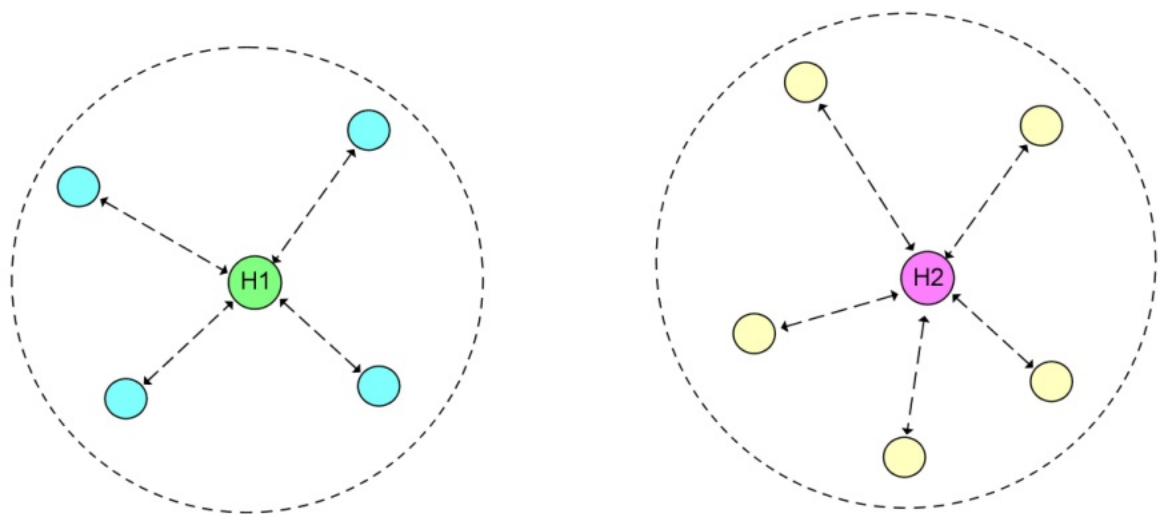

Figure 15. Network Topology

To provide or support time reference allocations a hub establishes a time base that divides the time into beacon periods (superframes). A hub transmits a beacon in each superframe, except in inactive superframes, or does not transmit a beacon in any superframe. A hub can operate in one of the following modes:

- Beacon mode with superframes
- Non-beacon mode with superframes
- Non-beacon mode without superframes

Fig. 16 shows the superframe structure when the hub operates in the beacon mode with superframes. A node can obtain, and initiate frame transactions, in the EAP1, RAP1, EAP2, RAP2, and CAP periods in any active superframe using CSMA/CA or slotted Aloha based random access protocols.
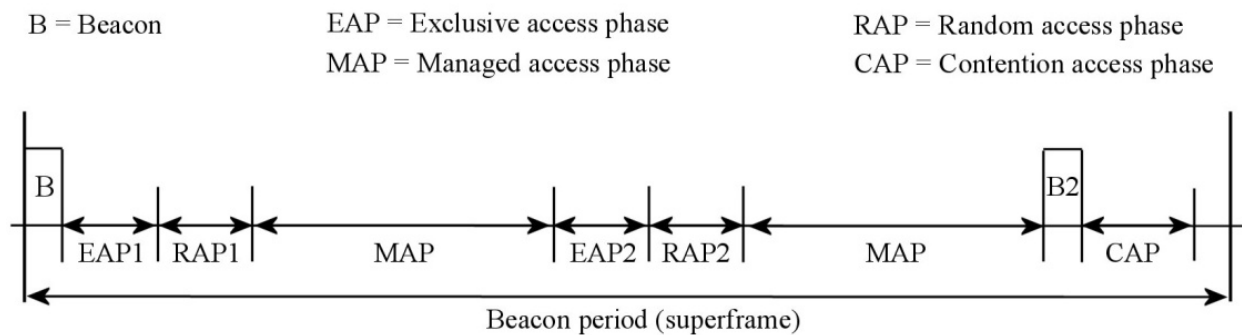

Figure 16. Layout of access phases in a superframe period for beacon mode

The EAP1 and EAP2 periods are used for the highest priority traffic, i.e. emergency information. The RAP1, RAP2, and CAP period are used for regular traffic. In a MAP period a hub can arrange scheduled uplink, downlink, and bilink allocation intervals. It can also provide unscheduled bilink allocation intervals.

In non-beacon mode with superframes the entire superframe period is a MAP phase. In the non-beacon mode without superframe boundaries the hub provides polled allocations whose length is specified in terms of the number of frames granted for transmission (type-II polled allocation).

According to this standard all nodes and hubs can choose the following three security levels:

- Level 0 – unsecured communications. The messages are transmitted in unsecured frames. There are no measures for data authentication and integrity validation, confidentiality and privacy protection, and replay defense.
- Level 1 – authentication only. Messages are transmitted in secured authenticated but not encrypted frames. Confidentiality and privacy is not supported.
- Level 2 – authentication and encryption. Messages are transmitted in secured authenticated and encrypted frames. Confidentiality, privacy protection, and replay defense are supported.

Security starts with a negotiation of the desired security suite between a node and a hub. Once the security selection is negotiated the two communicating parties activate a pre-shared or generate a new shared master key (MK).

7. Future research directions

The UWB channel has been measured and modelled extensively in recent years. Experimental WBANs using this technology have been developed and studied. Now that standards are in place the expectations, for the near future, is to have actual deployment of UWB BANs in medical environments.

Commercial applications of UWB have been limited to situations where precise localization is needed. Once medical applications are deployed the excellent ranging characteristics of the UWB signals could also be used to localize patients and medical equipment.

More experimental work is needed to learn the capabilities of UWB to directly monitor human organ functions as well as the workings of medical implants. In addition to experimental work, there is the need to develop accurate mathematical models that can be used in simulation studies as well as in 3D immersion systems.

Assuming UWB WBANs are widely deployed long term future applications is their use to extend their range and data delivery capabilities by having the BANs work in a cooperative fashion (Kaveh et al., 2011).

8. Summary

This chapter describes features of the UWB channel that should be taken into account when it is being considered for medical applications, in particular in hospital scenarios. These scenarios include cases where the human body is in motion. Using actual measurements mathematical models of the channel have been proposed.

It is also possible to use UWB technology to measure the workings of medical implants or body activities. This chapter presents the case of the response of an artificial aortic valve to UWB waves and its potential use to evaluate the working status of the valve.

Finally there is a brief discussion of engineering standards applicable to the use of UWB technology in the medical field.

Author details

Carlos Pomalaza-Ráez and Attaphongse Taparugssanagorn
Centre for Wireless Communications, University of Oulu, Finland

9. References

Fort A.; Ryckaert, J.; Desset, C.; De Doncker, P.; Wambacq, P.; & Van Biesen, L. (2006). Ultra-Wideband Channel Model for Communication Around the Human Body, *IEEE Journal*

on Selected Areas in Communications, vol. 24, No. 4, (April 2006), pp. 927-933, ISSN: 0733-8716.

IEEE 804.15.4 Standard (2011). Low-Rate Wireless Personal Area Networks (LR-WPANs).

IEEE 804.15.6 Standard (2012). Wireless Body Area Networks.

Ghaboosi K.; Pahlavan K.; & Pomalaza-Ráez C. (2011). A Cooperative Medical Traffic Delivery Mechanism for Multi-hop Body Area Networks, *Proceedings of the 2011 IEEE 22nd International Symposium on Personal Indoor and Mobile Radio Communications (PIMRC)*, ISBN: 978-1-4577-1348-4, Toronto, Canada, September 11-14, 2011.

Hentilä L.; Taparugssanagorn A.; Viittala H.; & Hämäläinen M. (2005). Measurement and modelling of an UWB channel at a hospital, *Proceedings of the International Conference on UWB ICUWB)*, ISBN: 0-7803-9397-X, Zurich, Switzerland, September 5-8, 2005.

Lazaro, A.; Girbau D. ; & Villarino R. (2010). Analysis of Vital Signs Monitoring Using an IR-UWB Radar, Progress in Electromagnetics Research, vol. 100, pp. 265-284, ISSN: 1070-4698.

Pancera, E.; Xuyang Li; Jalilvand, M.; Zwick, T.; & Wiesbeck, W. (2011). UWB medical diagnostic: in-body transmission modeling and applications, *Proceedings of the 5th European Conference on Antennas and Propagation* (EUCAP), ISBN: 978-1-4577-0250-1, Rome, Italy, April 11-15, 2011.

Taparugssanagorn A.; Pomalaza-Ráez C.; Isola A.; Tesi R.; Hämäläinen M.; & Iinatti J. (2010). Channel Modelling for Wireless Body Area Networks in Medical Applications, *Proceedings of the Third International Symposium on Medical Information & Communication Technology* (ISMICT), Montreal, Canada, February 24-26, 2009

Taparugssanagorn A.; Pomalaza-Ráez C.; Tesi R.; Hämäläinen M.; & Iinatti J. (2010). UWB Channel Modelling for Wireless Body Area Networks in a Hospital, *International Journal of Ultra Wideband Communications and Systems* (IJUWBCS) , vol. 1, No. 4, pp. 226-236, 2010, ISSN: 1758-7298.

Taparugssanagorn A.; Zhen B.; Tesi R.; Hämäläinen M.; Iinatti J; & Kohno R. (2011). A UWB WBAN channel model based on a pseudo-dynamic measurement, Annals of Telecommunications, vol. 66, No. 3-4, pp. 177-185, DOI: 10.1007/s12243-010-0228-5.

Viittala H.; Hämäläinen M.; Iinatti J.; & Taparugssanagorn A. (2009). Different experimental WBAN channel models and IEEE802.15.6 models: comparison and effects, *Proceedings of the 2nd International Symposium on Applied Sciences in Biomedical and Communication Technologies* (ISABEL 2009), E-ISBN: 978-1-4244-4641-4, Bratislava, Slovakia, November 24-27, 2009.

Yang W.; Sayrafian-Pour K.; Hagedorn J.; Terrill J.; Yazdandoost K.; Taparugssanagorn A.; Hämäläinen M.; & Iinatti J. (2011). Impact of an Aortic Valve Implant on Body Surface UWB Propagation: A Preliminary Study, *Proceeding of the Fifth International Symposium on Medical Information and Communication Technology* (ISMICT), ISBN: 9-781424-494446, Montreux, Switzerland, March 27-30, 2011.

Yazdandoost K. & Sayrafian-Pour K. (2009). Channel Model for Body Area Network (BAN), *Report to the IEEE*, P802.15. ID: IEEE 802.15-08-0780-02-0006, April 2009.